

# Coexistence of superconductivity and ferromagnetism in $\text{Sr}_{0.5}\text{Ce}_{0.5}\text{FBiS}_2$

Lin Li<sup>1</sup>, Yuke Li<sup>1,\*</sup>, Yuefeng Jin<sup>1</sup>, Haoran Huang<sup>1</sup>, Bin Chen<sup>1</sup>, Xiaofeng Xu<sup>1</sup>, Jianhui Dai<sup>1</sup>, Li Zhang<sup>3</sup>, Xiaojun Yang<sup>2</sup>, Huifei Zhai<sup>2</sup>, Guanghan Cao<sup>2</sup> and Zhuan Xu<sup>2</sup>

<sup>1</sup>*Department of Physics, Hangzhou Normal University,  
Hangzhou 310036, China*

<sup>2</sup>*State Key Lab of Silicon Materials and Department of Physics,  
Zhejiang University, Hangzhou 310027, China*

<sup>3</sup>*Department of Physics, China Jiliang University,  
Hangzhou 310018, China*

(Dated: February 4, 2015)

Through the combination of X-ray diffraction, electrical transport, magnetic susceptibility, and the heat capacity measurements, we studied the effect of Ce doping in the newly discovered  $\text{SrFBiS}_2$  system. It is found that  $\text{Sr}_{0.5}\text{Ce}_{0.5}\text{FBiS}_2$  undergoes a second-order transition below  $\sim 7.5$  K, followed by a superconducting transition with the critical temperature  $T_c \sim 2.8$  K. Our transport, specific heat and DC-magnetization results suggest the presence of bulk ferromagnetic correlation of Ce ion below 7.5 K that coexist with superconductivity when the temperature is further lowered below 2.8 K.

PACS numbers: 74.70.Xa, 74.25.Dw, 75.50.Lk

## I. INTRODUCTION

The fascinating relationship between superconductivity (SC) and magnetic ordering has been a central issue in condensed matter physics for several decades. It has been generally believed that within the context of the Bardeen-Cooper-Schrieffer (BCS) theory, the conduction electrons cannot be ordered magnetically and superconducting simultaneously<sup>1</sup>. In other words, superconductivity and magnetism are two antagonistic phenomena. Even though the superconducting pairing in cuprates, heavy fermions and Fe-based superconductors is mediated by antiferromagnetic spin fluctuations<sup>2,3</sup>, SC can be generally induced by suppressing the magnetic ordering with chemical doping or pressure<sup>4,5</sup>. Accordingly, the evidence for the coexistence of superconductivity and ferromagnetism (FM) in the same system is very rare and has only been claimed in a few compounds ( $\text{UGe}_2$ ,  $\text{URhGe}$ ,  $\text{EuFe}_2\text{As}_{2-x}\text{P}_x$ )<sup>6-9</sup>.

Recently, superconductivity with a transition temperature ( $T_c$ ) of 8.6 K in a novel  $\text{BiS}_2$ -based superconductor  $\text{Bi}_4\text{O}_4\text{S}_3$  has been discovered<sup>10</sup>. Immediately after this finding, several other  $\text{BiS}_2$ -based superconductors,  $\text{LnO}_{1-x}\text{F}_x\text{BiS}_2$  ( $\text{Ln}=\text{La}, \text{Ce}, \text{Pr}, \text{Nd}$ )<sup>11-15</sup> with the highest  $T_c$  of 10 K have been intensively studied. In analogy to cuprates and iron-based superconductors, the  $\text{BiS}_2$ -based compounds also possess a layered crystal structure consisting of superconducting  $\text{BiS}_2$  layers intercalated with various block layers, e.g.,  $\text{Bi}_4\text{O}_4(\text{SO}_4)_{1-x}$  or  $[\text{Ln}_2\text{O}_2]^{2-}$ . Apparently, the common  $\text{BiS}_2$  layer is believed to be the key structural element in search for a new superconductor, where superconductivity can be induced by chemical doping into the intercalated block layers. Indeed, through the replacement of  $\text{LaO}$  layer by  $\text{SrF}$  block, a new  $\text{BiS}_2$ -based superconductor  $\text{Sr}_{1-x}\text{La}_x\text{FBiS}_2$ , which is iso-structural to  $\text{LaOBiS}_2$ , has been successfully synthesized and studied<sup>16-18</sup>. The parent compound

$\text{SrFBiS}_2$  shows semiconducting-like behaviors, and the substitution of La into Sr site can induce  $T_c$  as high as 2.8 K.

Up to now, most studies on  $\text{LnOBiS}_2$ -based system have been focused on their electronic structure<sup>19</sup>, superconducting transition temperature<sup>20</sup> and the pairing symmetry<sup>21-23</sup>. Although most experimental studies<sup>24-26</sup> and theoretical calculations<sup>21,22</sup> seem to support the conventional  $s$ -wave pairing in these systems, the coexistence of superconductivity and ferromagnetism was recently proposed for the  $\text{CeO}_{1-x}\text{F}_x\text{BiS}_2$  superconductor<sup>14,27</sup>, which is apparently beyond the conventional BCS framework. In this paper, we demonstrate another example where the superconductivity is in close proximity to the ferromagnetism. We report a successful synthesis of Ce-doped  $\text{Sr}_{0.5}\text{Ce}_{0.5}\text{FBiS}_2$  superconductor, in which the diluted Ce ions order ferromagnetically at 7.5 K, and the system becomes superconducting below  $\sim 3$  K.

## II. EXPERIMENTAL

The polycrystalline sample  $\text{Sr}_{0.5}\text{Ce}_{0.5}\text{FBiS}_2$  was synthesized by two-step solid state reaction method. The starting materials, the high purity ( $\geq 99.9\%$ )  $\text{Ce}_2\text{S}_3$ ,  $\text{SrF}_2$ ,  $\text{CeF}_3$ ,  $\text{Bi}_2\text{S}_3$  and S powders, were weighted according to their stoichiometric ratio and then fully ground in an agate mortar. The mixture of powder was then pressed into pellets, heated in an evacuated quartz tube at 1073 K for 24 hours and finally quenched to room temperature. In order to get the pure and homogeneous phase, the sample is annealed at 973 K for 10h again. Crystal structure characterization was performed by powder X-ray diffraction (XRD) at room temperature using a D/Max-rA diffractometer with  $\text{Cu K}\alpha$  radiation and a graphite monochromator. The XRD data were col-

lected in a step-scan mode for  $10^\circ \leq 2\theta \leq 120^\circ$ . Lattice parameters were obtained by Rietveld refinements. The electrical resistivity was measured with a standard four-terminal method covering temperature range from 0.4 to 300 K in a commercial Quantum Design PPMS-9 system with a  $^3\text{He}$  refrigeration insert. The measurements of specific heat were also performed in this system. D.C. magnetic properties were measured on a Quantum Design Magnetic Property Measurement System (MPMS-7).

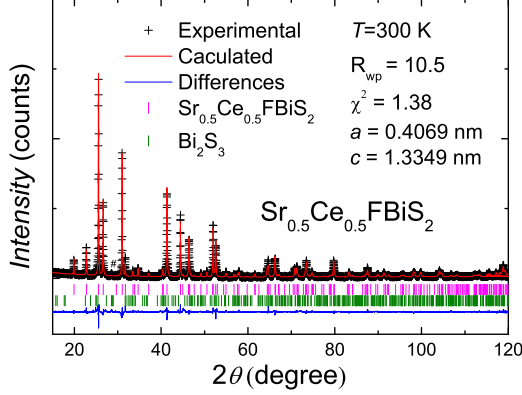


FIG. 1. (Color online) (a) Powder X-ray diffraction patterns and the Rietveld refinement profile for  $\text{Sr}_{0.5}\text{Ce}_{0.5}\text{FBiS}_2$  samples at room temperature. The # peak positions designate the impurity phase of  $\text{Bi}_2\text{S}_3$ .

### III. RESULTS AND DISCUSSION

Figure 1 shows the powder XRD patterns of the  $\text{Sr}_{0.5}\text{Ce}_{0.5}\text{FBiS}_2$  sample at room temperature, as well as the result of the Rietveld structural refinement. Overall, the main diffraction peaks of this sample can be well indexed based on a tetragonal cell structure with the  $P4/nmm$  space group. In addition to principal phase, extra minor peaks arising from impurity phase of  $\text{Bi}_2\text{S}_3$  with  $Pnma$  symmetry can also be observed<sup>28</sup>, and its content is estimated to be about 6% by Rietveld refinement. The refined lattice parameters are extracted to be  $a = 4.0695\text{\AA}$  and  $c = 13.3491\text{\AA}$ , which are shortened by 0.32% and 3.3% respectively, compared with those of parent compound  $\text{SrFBiS}_2$ <sup>16</sup>. As a result, the cell volume shrinks by 3.9% for  $\text{Sr}_{0.5}\text{Ce}_{0.5}\text{FBiS}_2$ . This result suggests that Ce ions were partially substituted to Sr ones.

Fig. 2(a) shows the temperature dependence of electrical resistivity ( $\rho$ ) under zero field and 9 T for  $\text{Sr}_{0.5}\text{Ce}_{0.5}\text{FBiS}_2$  sample. Its zero field resistivity increases monotonously with decreasing temperature but its value drops by several orders of magnitude compared to the un-doped sample<sup>16</sup>. Meanwhile, it also shows thermally activated behavior with decreasing tempera-

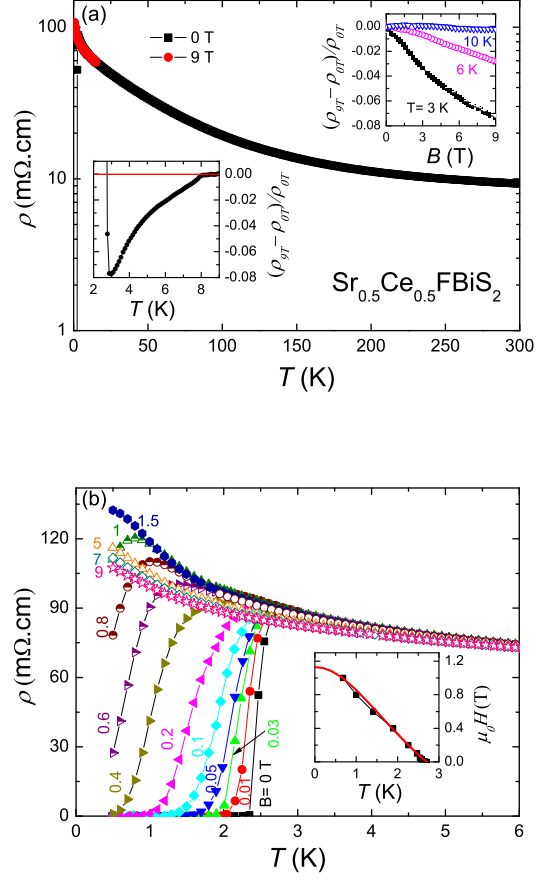


FIG. 2. (Color online) (a) Temperature dependence of resistivity ( $\rho$ ) for the  $\text{Sr}_{0.5}\text{Ce}_{0.5}\text{FBiS}_2$  samples under zero field and 9 T; The upper inset shows the field dependence of magnetoresistance for  $\text{Sr}_{0.5}\text{Ce}_{0.5}\text{FBiS}_2$  sample under several fixed temperatures ( $T = 3, 6, 10$  K). The lower one shows enlarged plot of magnetoresistance around  $T_{FM}$ . (b) Temperature dependence of (magneto-)resistivity for  $\text{Sr}_{0.5}\text{Ce}_{0.5}\text{FBiS}_2$  sample under several constant magnetic fields; The inset shows the  $\mu_0 H_{c2}$  as a function of temperature.

ture from 300 K. Using the thermal activation formula  $\rho(T) = \rho_0 \exp(E_a/k_B T)$  to fit  $\rho(T)$  at the temperature range from 120 K to 300 K, we obtain the thermal activation energy ( $E_a$ ) of  $\sim 22.1$  meV, which is far smaller than that of the undoped  $\text{SrFBiS}_2$  sample (38.2 meV)<sup>16,17</sup>, suggesting the decrease of gap size due to electron doping. With further cooling down, a sharp superconducting transition with  $T_c$  of 2.8 K, developing from a semiconducting-like normal state, is clearly observed. This feature is commonly observed in  $\text{BiS}_2$ -based superconductors<sup>11–15</sup>. As the magnetic field ( $H$ ) increases to 9 T, superconductivity is completely suppressed. The normal state recovered by the magnetic field is semiconducting-like down to 0.5 K. On closer examination, as shown in the lower inset of Fig. 2(a), the

negative magnetoresistance can be clearly observed below 7.5 K, and reaches  $\sim -8\%$  at 3 K, which will be discussed further below. The similar behaviors are also observed in the FM superconductors  $\text{EuFe}_2\text{As}_{2-x}\text{P}_x$ <sup>8</sup> and  $\text{CeO}_{0.95}\text{F}_{0.05}\text{FeAs}_{1-x}\text{P}_x$ <sup>9</sup>. As a comparison, no significant magnetoresistance was found in the parent compound  $\text{SrFBiS}_2$ <sup>17</sup> and  $\text{Sr}_{1-x}\text{La}_x\text{FBiS}_2$ <sup>16,18</sup>, and only small positive magnetoresistance due to the impurity phase Bi was reported in  $\text{Bi}_4\text{O}_4\text{S}_3$  system above  $T_c$ <sup>29</sup>. The magnetic field dependence of magnetoresistance under several different temperatures above  $T_c$  is plotted in the upper inset of Fig.2 (a). The negative magnetoresistance for  $T = 3$  K is clearly observed and almost reaches  $-8\%$  under  $B = 9$  T, decreases gradually and then disappears with increasing temperature to 10 K. This feature can be tentatively attributed to the FM ordering of  $\text{Ce}^{3+}$  moments (to be shown below).

Figure 2b shows the enlarged low- $T$  resistivity for  $\text{Sr}_{0.5}\text{Ce}_{0.5}\text{FBiS}_2$  sample under various magnetic fields below 6 K. With the application of magnetic fields, the superconducting transition becomes broadened and  $T_c$  decreases towards lower temperatures. Superconductivity is suppressed down to 0.7 K by a magnetic field as low as 1 T, and disappears at 1.5 T. Meanwhile, its resistivity displays semiconducting-like feature. With further increasing the magnetic field to 9 T, the negative magnetoresistance is observed in the normal state, consistent with the magnetoresistivity data as shown in Fig. 2(a). The similar result is also observed in  $\text{EuFe}_2\text{As}_{2-x}\text{P}_x$  superconductor<sup>8</sup>, which was reported to be a rare ferromagnetic superconductor. The inset of Fig.2(b) displays the upper critical field  $\mu_0 H_{c2}(T)$ , determined by using 90% normal state resistivity criterion, as a function of temperature. The  $\mu_0 H_{c2} - T$  diagram shows nearly linear dependence in the measured temperature range. According to Ginzburg-Landau theory, the upper critical field  $H_{c2}$  evolves with temperature following the formula:

$$H_{c2}(T) = H_{c2}(0)(1 - t^2)/(1 + t^2), \quad (1)$$

where  $t$  is the renormalized temperature  $T/T_c$ . The upper critical field  $H_{c2}$  estimated to be 1.16 T at  $T=0$  K, which is far smaller than that of Pauli paramagnetic limit  $\mu_0 H_p = 1.84T_c = 5$  T.

Figure 3(a) shows the temperature dependence of dc magnetic susceptibility for  $\text{Sr}_{0.5}\text{Ce}_{0.5}\text{FBiS}_2$  under  $B = 2$  T from 2 K to 300 K. The magnetic susceptibility above 100 K follows a modified Curie-Weiss behavior and can be fitted to  $\chi = \chi_0 + C/(T - \theta)$ , where  $\chi_0$  denotes the temperature-independent term,  $C$  is the Curie-Weiss constant and  $\theta$  denotes the paramagnetic Curie temperature. By subtracting the temperature-independent term ( $\chi_0$ ), the  $(\chi - \chi_0)^{-1}$  vs.  $T$ , as plotted in Fig.3(a), shows a linear behavior above 100 K. The fitting yields  $C = 0.80$  emu-K/mol-Ce and  $\theta = -19.2$  K. The effective magnetic moment  $\mu_{eff}$  is thus calculated to be  $2.53 \mu_B/\text{Ce}$ , close to the theoretical value of  $2.54\mu_B$  for a free  $\text{Ce}^{3+}$  ion.

To further investigate the coexistence of superconductivity and ferromagnetism in this sample, the magnetic

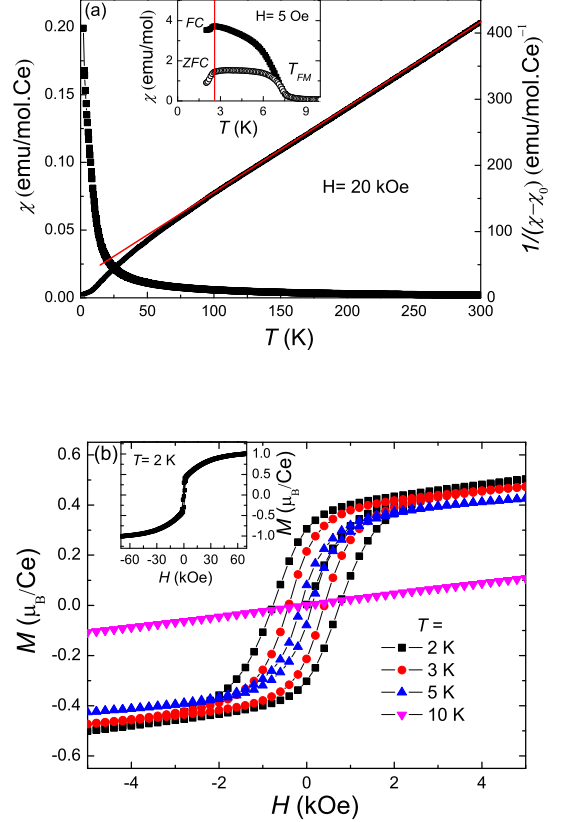


FIG. 3. (Color online) (a) Temperature dependence of magnetic susceptibility under  $H = 20$  kOe for  $\text{Sr}_{0.5}\text{Ce}_{0.5}\text{FBiS}_2$ . The inset shows the ZFC (open symbols) and FC (solid symbols) susceptibilities under  $H = 5$  Oe. (b) Isothermal magnetization of  $\text{Sr}_{0.5}\text{Ce}_{0.5}\text{FBiS}_2$  sample at several different temperatures.

susceptibility under 5 Oe with both zero-field-cooling (ZFC) and field-cooling (FC) modes below 10 K is depicted as the inset of Fig. 3(a). A rapid increase in the magnetic susceptibility and the obvious separation between ZFC and FC curves below 7.5 K may be ascribed to the long-range FM order of the Ce  $4f$  ions, or the possible small ferromagnetic clusters<sup>30</sup>. With further cooling down, an obvious drop around 2.8 K in both the ZFC and FC data is observed owing to the superconducting screening and Meissner effect, respectively. These results imply the coexistence of superconductivity and FM ordering in the system. Noted that the ZFC-FC hysteresis is slightly different to the case of a pure ferromagnetic system, suggesting a possibility for the existence of inter-cluster ferromagnetic interactions. The isothermal magnetization hysteresis loops for several temperatures are observed in Fig. 3(b). The clear hysteresis loop indicates a ferromagnetic-like order at 2 K on the sample. Moreover, the size of loop gradually shrinks with increasing temperatures, and then disappears at 10 K. At higher

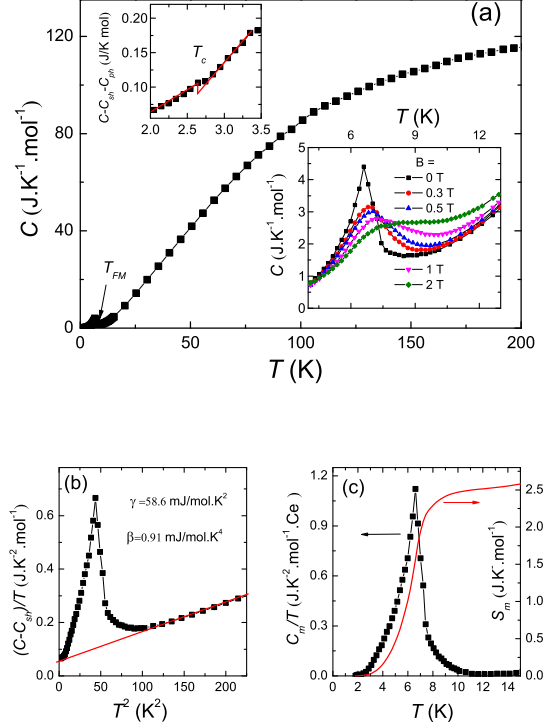


FIG. 4. (Color online) (a) Temperature dependence of specific heat for  $\text{Sr}_{0.5}\text{Ce}_{0.5}\text{FBiS}_2$  under zero field below 200 K. The upper left panel shows the specific heat anomaly at 2.8 K because of the superconducting transition. The lower right panel shows the magnetic specific-heat anomaly around 7.5 K under several magnetic fields. (b) The  $C/T$  vs.  $T^2$  at low-T region (the dashed line obeys  $C/T = \gamma + \beta T^2$ ). (c) The temperature dependence of the  $C_m/T$  (where  $C_m$  denotes magnetic contribution to the specific heat) and entropy  $S_m$ .

magnetic fields for  $T = 2$  K, the magnetization increases monotonously and then tends to saturate, as shown in inset of Fig. 3(b). The largest saturated magnetic moment estimated is about  $0.95 \mu_B$ , close to the  $1 \mu_B$  expected for a  $\text{Ce}^{3+}$  doublet ground state because of the crystal field effect, similar to those of in  $\text{CeFe}(\text{Ru})\text{PO}$ <sup>31,32</sup> and  $\text{CeO}_{0.95}\text{F}_{0.05}\text{FeAs}_{1-x}\text{P}_x$ <sup>9</sup> compounds with ferromagnetic correlation.<sup>9,32</sup> It is worth noting that this hysteresis loop has not been reported thus far in other  $\text{BiS}_2$ -based superconductors, even in the  $\text{CeO}_{1-x}\text{F}_x\text{BiS}_2$  system<sup>27</sup>.

The specific heat measurement of  $\text{Sr}_{0.5}\text{Ce}_{0.5}\text{FBiS}_2$  sample was plotted in Fig. 4. The  $C(T)$ , in Fig.4 (a), shows a Dulong-Petit law and saturates to the classical limit of  $3NR \sim 120 \text{ J K}^{-1} \text{ mol}^{-1}$  at high temperature, where  $N$  denotes the number of elements per fu. A clear  $\lambda$ -shaped kink at  $\sim 7.5$  K is observed, strongly demonstrating the second order phase transition. With increasing magnetic field, the anomaly shifts to higher temperature and becomes rather broadened, consistent with a FM nature of the transition, as shown in the

lower inset of Fig. 4 (a). Reminiscent of the features in the magnetic susceptibility and resistivity data around this temperature, the heat capacity anomaly is ascribed to the ferromagnetic ordering of Ce moments. However, through subtracting the fitted results from the raw data, a specific heat anomaly associated with the superconducting transition is detected below  $T_c$  in the upper inset of Fig.4 (a). The jump,  $\Delta C$  at  $T_c$ , is much weaker than that of the other  $\text{BiS}_2$ -based superconductors<sup>16</sup>, suggesting that the superconducting jump has been reduced by the magnetic signal. It has been reported that both  $\text{CeO}_{0.5}\text{F}_{0.5}\text{BiS}_2$  and  $\text{YbO}_{0.5}\text{F}_{0.5}\text{BiS}_2$  with magnetic rare earth elements do not show any anomalies around  $T_c$  in the specific heat data<sup>34</sup>, while the clear jump is always observed in the systems with non-magnetic elements, such as  $\text{Sr}_{0.5}\text{La}_{0.5}\text{FBiS}_2$ ,  $\text{LaO}_{1-x}\text{F}_x\text{OBiS}_2$  and  $\text{La}_{1-x}\text{M}_x\text{OBiS}_2$ <sup>16,35</sup> whose normal state is paramagnetic. These results suggest that the anomaly around  $T_c$  may be overwhelmed by the enhanced specific heat signal arising from the contribution of magnetic moments.

To further analyze the specific heat data below 15 K, the specific heat can be written as  $C = \gamma T + \beta T^3 + C_{mag} + C_{sch}$ , where  $\gamma$  is the Sommerfeld coefficient,  $C_{mag}$  and  $C_{Ph} = \beta T^3$  represent the magnetic and phonon contributions, and  $C_{sch}$  is equal to  $\alpha/T^2$ , representing the Schottky anomaly item. We first fit the low- $T$  specific heat below 3 K to obtain the Schottky anomaly item ( $C_{sch}$ ) due to the contributions of nuclear spins. By subtracting the  $C_{sch}$  from the total specific heat, the  $C/T$  versus  $T^2$  shows a linear behavior from 10 to 15 K, yields values of  $\gamma = 58.6 \text{ mJ/mol.K}^2$  and the Debye temperature  $\Theta = 220$  K, as shown in the Fig.4(b). This value falls in between those for  $\text{CeO}_{0.5}\text{F}_{0.5}\text{BiS}_2$  (224 K) and  $\text{YbO}_{0.5}\text{F}_{0.5}\text{BiS}_2$  (186 K)<sup>34</sup>. Considering that only 50% Ce are doped into the lattice, the  $\gamma$  value should be  $117.2 \text{ mJ/K}^2 \cdot \text{mol} \cdot \text{Ce}$  for the Ce end compound, which is enhanced by a factor of 50-80 compared to those of  $\text{Sr}_{0.5}\text{La}_{0.5}\text{FBiS}_2$  ( $1.42 \text{ mJ/mol K}^2$ )<sup>18</sup> and  $\text{La}_{1-x}\text{M}_x\text{OBiS}_2$  ( $M=\text{Ti, Zr, Th}$ ) ( $0.58\text{-}2.21 \text{ mJ/mol K}^2$ )<sup>35</sup>. The substantially enhanced  $\gamma$  may be mainly originating from the electronic correlation effect from Ce-4*f* electrons. The magnetic contribution  $C_{mag}$  was obtained by removing the contributions of electronic,  $C_{Ph}$  and  $C_{sch}$ . The magnetic entropy estimated associated with the ferromagnetic ordering is  $2.7 \text{ J/K mol Ce}$  around 10 K, which amounts to 50% of  $R \ln(2J+1)$  with  $J=1/2$  for  $\text{Ce}^{3+}$  ions below 15 K, as shown in the Fig.4 (c). Considered omission of magnetic entropy, the  $S_m$  value actually should be close to the limit of the  $\text{Ce}^{3+}$ . These results indicate that the superconductivity coexists with a bulk ferromagnetic-like order in the sample.

Thus far, a growing body of evidence for the coexistence of superconductivity and ferromagnetism has been reported. The vast majority of these systems show superconductivity before the ferromagnetic ordering, and lead to the re-entrant superconductivity overlapped with a magnetic phase, such as  $\text{ErRh}_4\text{B}_4$ <sup>36</sup>,  $\text{ErNi}_2\text{B}_2\text{C}$ <sup>37</sup>,  $\text{EuFe}_2\text{As}_{2-x}\text{P}_x$ <sup>8</sup>. In those systems, two separate sets of electrons may be responsible for magnetic ordering

and superconductivity, respectively. While in our case, the ferromagnetic transition temperature is substantially higher than  $T_c$ . The role of Ce doping is twofold, they provide carriers to BiS<sub>2</sub> layers inducing superconductivity and they ferromagnetically order in the (Sr,Ce)F sublattice. Compared with the previous reports<sup>8,27</sup>, the remarkable feature here is that the FM ordering can be established in the diluted Ce lattice (50% Ce in the SrF layer) mainly due to the RKKY interaction. More experiments (neutron and NMR) and theoretical insight may provide useful clues for this issue in BiS<sub>2</sub>-based superconductors.

#### IV. CONCLUSION

In summary, by partially substituting Ce for Sr in the newly discovered SrFBiS<sub>2</sub> system, a ferromagnetic-like bulk ordered phase was put in evidence for tempera-

tures below 7.5 K by transport, specific heat and DC-magnetization measurements. Interestingly, this magnetic phase due to Ce<sup>3+</sup> order coexists with superconductivity as temperature is lowered below  $T_c=2.8$  K. In this system Ce substitution likely provides carriers to the superconducting BiS<sub>2</sub> layers and, at the same time, it induces a FM ordering in the blocking (Sr,Ce)F layers.

*Note:* After the completion of this work, we became aware of the recent paper<sup>38</sup>, which also observed SC in Sr<sub>1-x</sub>Ln<sub>x</sub>FBiS<sub>2</sub> ( $Ln = \text{Ce, Pr, Nd, Sm}$ ) systems.

#### ACKNOWLEDGMENTS

Yuke Li would like to thank Yongkang Luo for inspiring discussions. This work is supported by the National Basic Research Program of China (Grant No. 2011CBA00103 and 2014CB921203), NSFC (Grant No. U1332209, 11104053, 11474080, and 61376094)

- 
- <sup>1</sup> N. F. Berk, and J. R. Schrieffer, Phys. Rev. Lett. **17**, 436 (1966).
  - <sup>2</sup> N. D. Mathur, Nature **394**, 39 (1998).
  - <sup>3</sup> D. J. Scalapino, Rev. Mod. Phys. **84**, 1383 (2012).
  - <sup>4</sup> Y. Kamihara, T. Watanabe, M. Hirano, and H. Hosono, J. Am. Chem. Soc. **130**, 3296 (2006).
  - <sup>5</sup> M. S. Torikachvili, S. L. Budko, N. Ni, and P. C. Canfield, Phys. Rev. Lett. **101**, 057006 (2008).
  - <sup>6</sup> S. S. Saxena, P. Agarwal, K. Ahilan, F. M. Grosche, R. K. W. Haselwimmer, M. J. Steiner, E. Pugh, I. R. Walker, S. R. Julian, P. Monthoux, G. G. Lonzarich, A. Huxley, I. Sheikin, D. Braithwaite, and J. Flouquet, Nature **406**, 587 (2000).
  - <sup>7</sup> D. Aoki, A. Huxley, E. Ressouche, D. Braithwaite, J. Flouquet, J. Brison, E. Lhotel, C. Paulsen, Nature **413**, 613 (2001).
  - <sup>8</sup> Z. Ren, Q. Tao, S. Jiang, C. Feng, C. Wang, J. Dai, G. Cao, and Z. Xu, Phys. Rev. Lett. **102**, 137002 (2009).
  - <sup>9</sup> Y. K. Luo, H. Han, S. Jiang, X. Lin, Y. K. Li, J. H. Dai, G. H. Cao, and Z. A. Xu, Phys. Rev. B **83**, 054501 (2011).
  - <sup>10</sup> Y. Mizuguchi, H. Fujihisa, Y. Gotoh, K. Suzuki, H. Usui, K. Kuroki, S. Demura, Y. Takano, H. Izawa, O. Miura, Phys. Rev. B **86**, 220510(R) (2012).
  - <sup>11</sup> Y. Mizuguchi, S. Demura, K. Deguchi, Y. Takano, H. Fujihisa, Y. Gotoh, H. Izawa, O. Miura, J. Phys. Soc. Jpn. **81** 114725 (2012).
  - <sup>12</sup> S. Demura, Y. Mizuguchi, K. Deguchi, H. Okazaki, H. Hara, T. Watanabe, S. J. Denholme, M. Fujioka, T. Ozaki, H. Fujihisa, Y. Gotoh, O. Miura, T. Yamaguchi, H. Takeya, and Y. Takano, J. Phys. Soc. Jpn. **82**, 033708 (2013).
  - <sup>13</sup> V.P.S. Awana, A. Kumar, R. Jha, S. Kumar, J. Kumar, and A. Pal, Solid State Communications **157**, 31 (2013).
  - <sup>14</sup> J. Xing, S. Li, X. Ding, H. Yang and H. H. Wen, Phys. Rev. B **86**, 214518 (2012).
  - <sup>15</sup> R. Jha, S. K. Singh, and V. P. S. Awana, J. Sup. and Novel Mag. **26**, 499 (2013).
  - <sup>16</sup> X. Lin, X. X. Ni, B. Chen, X. F. Xu, X. X. Yang, J. H. Dai, Y. K. Li, X. J. Yang, Y. K. Luo, Q. Tao, G. H. Cao, and Z. A. Xu, Phys. Rev. B **87** 020504 (2013).
  - <sup>17</sup> H. C. Lei, K. F. Wang, M. Abeykoon, E. S. Bozin, and C. Petrovic, Inorg. Chem. **52**, 10685 (2013).
  - <sup>18</sup> Y. K. Li, X. Lin, L. Li, N. Zhou, X. F. Xu, C. Cao, J. H. Dai, L. Zhang, Y. K. Luo, W. H. Jiao, Q. Tao, G. H. Cao and Z. Xu, Supercond. Sci. Technol. **27** 035009 (2014).
  - <sup>19</sup> B. Li, Z. W. Xing, and G. Q. Huang, arXiv: 1210.1743
  - <sup>20</sup> C. T. Wolowiec, B. D. White, I. Jeon, D. Yazici, K. Huang, and M. B. Maple, J. Phys.: Condens. Matter **25**, 422201 (2013).
  - <sup>21</sup> Y. Liang, X. Wu, W. F. Tsai, and J. P. Hu, Front. Phys. **9**, 194 (2014).
  - <sup>22</sup> T. Yildirim, Phys. Rev. B **87**, 020506(R) (2013).
  - <sup>23</sup> G. B. Martins, A. Moreo, and E. Dagotto, Phys. Rev. B **87**, 081102(R) (2013).
  - <sup>24</sup> G. Lamura, T. Shiroka, P. Bonfa, S. Sanna, R. De Renzi, C. Baines, H. Luetkens, J. Kajitani, Y. Mizuguchi, O. Miura, K. Deguchi, S. Demura, Y. Takano, and M. Putti, Phys. Rev. B **88**, 180509 (2013).
  - <sup>25</sup> L. K. Zeng, X. B. Wang, J. Ma, P. Richard, S. M. Nie, H. M. Weng, N. L. Wang, Z. Wang, T. Qian, and H. Ding, Phys. Rev. B **90**, 054512 (2014).
  - <sup>26</sup> Z. R. Ye, H. F. Yang, D. W. Shen, J. Jiang, X. H. Niu, D. L. Feng, Y. P. Du, X. G. Wan, J. Z. Liu, X. Y. Zhu, H. H. Wen, and M. H. Jiang, Phys. Rev. B **90**, 045116 (2014).
  - <sup>27</sup> S. Demura, K. Deguchi, Y. Mizuguchi, K. Sato, R. Honjyo, A. Yamashita, T. Yamaki, H. Hara, T. Watanabe, S. J. Denholme, M. Fujioka, H. Okazaki, T. Ozaki, O. Miura, T. Yamaguchi, H. Takeya, and Y. Takano, arXiv: 1311.4267
  - <sup>28</sup> B. Chen, C. Uher, L. Iordanidis, and M. G. Kanatzidis, Chem. Mater. **9**, 1655 (1997).
  - <sup>29</sup> S. Li, H. Yang, J. Tao, X. Ding, and H. H. Wen, Sci. China-Phys. Mech. Astron. **56**, 2019 (2013).
  - <sup>30</sup> R. P. Panmand, M. V. Kulkarni, M. Valant, S. W. Gosavi, and B. B. Kale, AIP Advances. **3**, 022123 (2013).
  - <sup>31</sup> C. Krellner, N. S. Kini, E. M. Bruning, K. Koch, H. Rosner, M. Nicklas, M. Baenitz, and C. Geibel, Phys. Rev. B **76**, 104418 (2007).
  - <sup>32</sup> E. M. Bruning, C. Krellner, M. Baenitz, A. Jesche, F. Steglich, and C. Geibel, Phys. Rev. Lett. **101**, 117206

- (2008)
- <sup>33</sup> S. X. Chi, D. T. Adroja, T. Guidi, R. Bewley, S. L. Li, J. Zhao, J.W. Lynn, C. M. Brown, Y. Qiu, G. F. Chen, J. L. Lou, N. L. Wang, and P. C. Dai, *Phys. Rev. Lett.* **101**, 217002 (2008)
- <sup>34</sup> D. Yazici, K. Huang, B. D. White, A. H. Chang, A. J. Friedman, and M. B. Maple, *Philosophical Magazine* **93**, 673 (2012).
- <sup>35</sup> D. Yazici, K. Huang, B. D. White, I. Jeon, V. W. Burnett, A. J. Friedman, I. K. Lum, M. Nallaiyan, S. Spagna, and M. B. Maple, *Phys. Rev. B* **87**, 174512 (2013).
- <sup>36</sup> W. A. Fertig, D. C. Johnston, L. E. DeLong, R. W. McCallum, M. B. Maple, and B. T. Matthias, *Phys Rev Lett* **38**, 987 (1977).
- <sup>37</sup> P. C. Canfield, S. L. Bud'ko, B. K. Cho, *Physica C* **262**, 249 (1996).
- <sup>38</sup> R. Jha, B. Tiwari, V.P.S. Awana, arXiv:1407.3105